Statistical *n*-Best AFD-Based Sparse Representation for ECG Biometric Identification

Chunyu Tan, Liming Zhang, *Member, IEEE*, Tao Qian, Susana Brás, and Armando J. Pinho, *Member, IEEE*

***Abstract*— Electrocardiogram (ECG) biometric recognition as a personal identification method is receiving more and more attention because it can support live verification results. Compared with other biometric-based methods, it can provide higher security performance. The difficulty of the problem lies in how to stably extract ECG signal features and achieve real-time verification. In this study, a new type of sparse representation learning framework called statistical *n*-best adaptive Fourier decomposition (SAFD) originated by Qian is adopted in ECG biometric identification. Adaptive Fourier decomposition (AFD) is a recently developed combination of transform-based signal decomposition and sparse representation method, which can adaptively select the atoms from a redundant dictionary through orthogonal processing. The advantage of the AFD-type methods is that each atom in the dictionary has a precise mathematical formula with good analytic properties. This characteristic is significantly distinguished it from other existing sparse representations, where the atoms learned are usually matrix data and cannot be described mathematically. The proposed SAFD extends the existing *n*-best AFD from processing single signal to multi-signals and implements the *n*-best AFD in the stochastic Hardy space. Therefore, the small number of learned atoms by SAFD is sufficient to capture internal structure and robustness of the signal and generate a discriminative representation that reflects the time–frequency characteristics of signals. It is very suitable for non-stationary signals like ECG. The proof of convergence of the algorithm is presented. Extensive experiments are conducted on five public databases collected in different realistic conditions, and an average identification accuracy of 98.0% is achieved. In addition, less than 1 ms for one matching process makes it possible to be implemented in real time. Experimental results demonstrate that the proposed method can achieve superior performance compared to other state-of-the-art ECG biometric identification methods.**

***Index Terms*— Biometric identification, electrocardiogram (ECG), sparse representation, statistical *n*-best adaptive Fourier decomposition (SAFD), time–frequency representation.**

I. Introduction

With the increasing use of technology to enhance human activities and improve human lifestyles, personal identification has become an indispensable part of human life nowadays. Traditional identification methods (including ID numbers, passwords, and tokens) have also become easily destroyed or stolen due to the development of technology [1]. As a promising option, biometric identification using human physiological or behavioral traits that are mostly unique between individuals is receiving more and more attention [2]. Typical biometric technologies, such as fingerprints, faces, iris, and voice, face the challenge of identity theft, because they can be the result of malicious forgery [3]. Compared with these existing biometric technologies, electrocardiogram (ECG) signals can only be collected and verified on-site. It is more difficult to replicate and forge, and thus, provides a reliable way for human authentication and unique recognition.

In the earliest study that applied ECG signals for human identification, Biel *et al.* [4] demonstrated the feasibility by employing 12-lead ECG signals to classify 20 subjects in 2001. Then, many related articles were proposed in the follow-up [5]–[8]. In the literature, ECG biometric identification systems can be divided into two categories: the fiducial-based and the non-fiducial-based methods [9]. The non-fiducial-based methods are commonly used for releasing fiducial points detection. There are three types in general, that is, transform-based, convolutional neural network (CNN)-based, and sparse representation-based methods. The transform-based methods use the features extracted through different mathematical transforms, including wavelet transform (WT) [10]–[13] and S-transformation [5]. The advantage of these methods is that the extracted features can be fully described mathematically, while the disadvantage is that the extracted features are usually redundant, resulting in unsatisfactory recognition performance. The currently widely used deep learning methods have achieved outstanding performance in many fields. However, its advantage, but also the disadvantage, is that it

Manuscript received May 28, 2021; revised September 10, 2021; accepted September 19, 2021. Date of publication October 8, 2021; date of current version October 25, 2021. This work was supported in part by the Science and Technology Development Fund of Macao Special Administrative Region (SAR) Fundo para o Desenvolvimento das Ciências e da Tecnologia (FDCT) under Grant 0123/2018/A3; in part by Multi-Year Research Grant 2018-00111-FST; in part by European Regional Development Fund, Fundo Social Europeu (FSE) through COMPETE2020, through Fundação para a Ciência e Tecnologia (FCT), in the scope of the Framework Contract Foreseen in the numbers 4–6 of the article 23, of the Decree-Law 57/2016, of August 29, changed by Law 57/2017, of July 19; and in part by the Scope of the Projects [Instituto de Engenharia Eletrónica e Informática de Aveiro/Universidade de Aveiro (IEETA/UA)] under Grant UIDB/00127/2020. The Associate Editor coordinating the review process was Priya Ranjan Muduli. *(Corresponding author: Liming Zhang.)*

Chunyu Tan is with the Faculty of Science and Technology, University of Macau, Macau, China, and also with the School of Artificial Intelligence, Anhui University, Hefei 230000, Anhui, China (e-mail: yb57416@connect.um.edu.mo).

Liming Zhang is with the Faculty of Science and Technology, University of Macau, Macau, China (e-mail: lmzhang@um.edu.mo).

Tao Qian is with Macao Center of Mathematical Sciences, Macau University of Science and Technology, Macau, China (e-mail: tqian@must.edu.mo).

Susana Brás and Armando J. Pinho are with the Institute of Electronics and Informatics Engineering of Aveiro (IEETA) and the Department of Electronics Telecommunications and Informatics (DETI), University of Aveiro, 3810-193 Aveiro, Portugal (e-mail: susana.bras@ua.pt; ap@ua.pt).

Digital Object Identifier 10.1109/TIM.2021.3119138

relies on a large amount of training data. The ECG biometric identification system needs to learn the features of each person individually, so the amount of the training data is limited [10]. Therefore, the robustness of deep learning in this field is greatly reduced [5], [14], [15].

Sparse representation uses a few representative atoms of dictionary to approximate the original signal. The representative features are also learned, but compared with deep learning, the training process only requires very little training data. For example, the training samples of 277 563 are used for training CNN in [16], while only 12 heartbeats per subject from a database with 47 subjects and a database with 89 subjects are used to train the dictionary of the sparse representation algorithm in [6]. Sparse representation has achieved very good performance in ECG biometric identification. Wang *et al.* [17] used sparse representation of local segments to extract compact and discriminative features from ECG signals for personal identification. Jaafar *et al.* [18] employed the kernel sparse representation classifier (KSRC) in the ECG biometric recognition system, to increase the system performance in high-dimensional feature spaces. In [19], a unified sparse representation that collaboratively exploited joint and specific patterns for ECG biometric recognition was developed. Xu *et al.* [20] proposed a structural sparse representation algorithm with class-specific dictionary for ECG biometric recognition.

In the literature, the dictionary atoms of the sparse representations are adaptively learned based on the signal. However, the extracted features are usually represented by matrix data and cannot be described mathematically. This shortcoming limits further analysis of ECG signals. In addition, the traditional sparse representation methods used for ECG biometric recognition mainly use the consistent constraints on all ECG signals to search for consistent representations, while ignoring the signal divergence of each subject [19]. Finally, the large dictionary dimension and large number of matrix calculations in the dictionary learning of traditional sparse representation methods lead to high computation complexity [19], especially for large databases. In practice, most traditional sparse representation methods are difficult to implement in real-time.

This article proposes a novel sparse representation learning framework called statistical n-best adaptive Fourier decomposition (SAFD) for ECG biometric identification. Adaptive Fourier decomposition (AFD) is a newly developed combination of transform-based signal decomposition and sparse representation method [21]–[23]. Unlike the other transform-based methods that use preselected fixed bases, AFD decomposes the signal according to the adaptive selection of atoms from a redundant dictionary through orthogonal processing. Unlike other sparse representation methods that have no mathematical description on the dictionary atoms, each atom in the AFD-based dictionary has a precise mathematical formula enjoying good analytic properties. In particular, the adaptive decomposition offers positive frequency decomposition as well as fast converges to the interested signal.

AFD has been proved to be a powerful tool for ECG signal compression [24], [25] and offers higher performance with its ability for signal modeling [26], [27]. The n-best AFD [22] is a variant of AFD, which uses the learning method to select n best atoms to represent the signal. Due to its optimization in the cyclic iteration, the dictionary atoms learned by n-best AFD are more robust and more effective to represent the signal. The existing n-best AFD is used to process only one signal at a time. To generalize the n-best AFD into processing multi-signals on stochastic analytic Hardy spaces, this article adopts the newly proposed SAFD theory [28] and proposes a novel learning framework and the algorithm based on SAFD, which is applied to ECG biometric identification. SAFD can extract common features from multi-signals at one time, thereby improving the effectiveness and efficiency of sparse representation. It has been successful applied in ECG classification [29]. Besides, the numbers of the common features from the multi-signals are less than the sum of the feature numbers from single signals, and therefore it also has potential applications in the fields of signal compression.

The main contributions of this article are summarized as follows.

1) The learning framework and algorithm of SAFD is introduced in this article. It extends the existing n-best AFD from processing single signal to multi-signals and implements the n-best AFD in the stochastic Hardy space. In addition to the ECG signal, the SAFD can also be generalized to other types of signals.
2) Due to the optimization nature, SAFD is more effective and stable to approximate signals with fast convergence. Only a few atoms are needed to represent the signal, which greatly enhances the sparsity. Though the extracted features are more compact, the sparse features effectively minimize intra-subject variability and maximize inter-subject variability of ECG signals and achieve the final robust and discriminative representation.
3) The extracted features represented by SAFD dictionary atoms can be described by time–frequency characteristics mathematically. The time–frequency structure of ECG signals provides relevant and effective pattern information for ECG biometric identification.
4) Compared with the other sparse representation methods, our method requires only a small amount of training data to find appropriate dictionary atoms to represent the interested signals. In addition, the fast convergence of the algorithm greatly reduces the calculation time. The efficient data calculation process can greatly save storage space. These advantages make the proposed ECG biometric system suitable for real-time implementation and provide great potential for the practical applications.
5) The proposed method is tested on five ECG databases, all publicly available. Four of them are currently used for the ECG biometric algorithm evaluation. The other one was designed to collect ECG data in three sessions, allowing the algorithm evaluation over different time periods.

The rest of the article is organized as follows. The proposed method is described in detail in Section II. In Section III, experimental results are presented. Finally, conclusions are drawn and future works are suggested in Section IV.

II. Principle of the Proposed SAFD

A. Mathematical Foundation

1) Preliminaries: As the proposed SAFD is through the n-best AFD, we will briefly introduce the fundamental knowledge of the n-best AFD. The n-best AFD is based on the n-orthogonal rational function system, or the n-Takenaka–Malmquist system (the n-TM system in brief). For a given set of $a_k \in \mathbb{D}$, where $k = 1, 2, \ldots, n$ and $\mathbb{D}$ is the unit disk, the n-TM system is denoted as $\{B_k\}$ [22] with

$$B_k(z) = B_{a_1,\ldots,a_k} = \frac{\sqrt{1-|a_k|^2}}{1-\bar{a}_k z}\prod_{j=1}^{k-1}\frac{z-a_j}{1-\bar{a}_j z} \tag{1}$$

and B_k are called *weighted Blaschke products (wBPs)*. A n-TM system is said to be adaptive if the parameters a_k for all k are selected according to the input signal. An adaptive n-TM system is a generalization of the *n-Fourier system*, the latter being composed of the monomials $\{z^k\}_{k=1}^n$, corresponding to $a_k = 0$ for all k in the n-TM system.

An element in the dictionary $\{e_a\}_{a\in\mathbb{D}}$

$$e_a = \frac{\sqrt{1-|a|^2}}{1-\bar{a}z} \tag{2}$$

is called an *evaluator* [21], which is employed to facilitate computation of energy gain during the parameter selection. A weight Blaschke product in (1) comes from a product of several evaluators with a proper normalization [21]. The evaluators are the reproducing kernels of the Hardy space $H^2(\mathbb{D})$.

The n-best AFD is the n-best approximation to an analytic signal in the Hardy space by a linear combination of some n dictionary atoms in a learned n-TM system, so as to achieve the sparsity. For an analytic signal $f \in H^2(\mathbb{D})$, the n-best AFD is a function of the form

$$\tilde{f}(z) = \sum_{k=1}^{n}(c_f)_k B_{a_1^f,\ldots,a_k^f} \tag{3}$$

which best approximates f under a selection of the n-tuple of the parameters $a_1^f, a_2^f, \ldots, a_n^f$. $(c_f)_k = \langle f, B_{a_1^f,\ldots,a_k^f}\rangle$ is the kth coefficient of $B_{a_1^f,\ldots,a_k^f}$, where $\langle\,,\rangle$ represents the inner product in $H^2(\mathbb{D})$. The existence and a proposed algorithm of (2) may be found in [22].

Extending the n-best AFD to the stochastic Hardy space, we get SAFD.

2) SAFD: The stochastic Hardy space is defined as follows:

$$H_\xi^2(\mathbb{D}) = \Bigg\{ x : \mathbb{D}\times\Omega\to\mathbb{C} \mid x(z,\xi) \text{ is a.s. analytic in } z$$
$$x(z,\xi) = \sum_{k=0}^{\infty} c_k(\xi) z^k \text{ with}$$
$$||x||_{\mathcal{N}}^2 = \sum_{k=0}^{\infty} E_\xi |c_k(\xi)|^2 < \infty \Bigg\} \tag{4}$$

where E_ξ stands for the mathematical expectation in the underlying probability space (Ω, μ), $\xi \in \Omega$. $||x||_{\mathcal{N}}$ is the energy expectation norm of x, and $\mathcal{N} = L_\xi^2(\partial\mathbb{D})$ is the space of random signals of finite energy. $x(z,\xi)$ in (4) can also be written as $x(t,\xi) = \Sigma_{k=0}^{\infty} c_k(\xi) e^{ikt}$ with $z = e^{it}$.

Let $y(t,\xi)$ be a real-valued signal in $L_\xi^2(\partial\mathbb{D})$. The associated analytic signals of $y(t,\xi)$ is denoted as

$$x(t,\xi) = \frac{1}{2}\big(y(t,\xi) + iHy(t,\xi) + c_0\big) \tag{5}$$

where c_0 is the 0th Fourier coefficient, and H is the Hilbert transformation.

Now $x(t,\xi)$ is in $H_\xi^2(\mathbb{D})$. Let $\bar{x} = E_\xi(x(t,\xi))$, we have

$$x(t,\xi) = \overline{x}(t) + r(t,\xi) \tag{6}$$

where r is the remainder. In fact, $\bar{x}$ is in $H^2(\mathbb{D})$.

Theorem 2.1: If $x(t,\xi) \in H_\xi^2(\mathbb{D})$, let $\bar{x} = E_\xi(x(t,\xi))$, then $\bar{x} \in H^2(\mathbb{D})$.

Proof: We will show

$$\bar{x} = E_\xi(x(t,\xi)) = \sum_{k=0}^{\infty} E_\xi(c_k(\xi)) z^k \tag{7}$$

and $\bar{x} \in H^2(\mathbb{D})$.

In fact, according to Parseval's inequality, we have $\|\sum_{k=0}^{\infty} E_\xi(c_k(\xi))z^k\| = (\sum_{k=0}^{\infty}|E_\xi(c_k(\xi))|^2)^{(1/2)}$, and according to the Minkovski's inequality, we have $(\sum_{k=0}^{\infty}|E_\xi(c_k(\xi))|^2)^{(1/2)} \le E_\xi[(\sum_{k=0}^{\infty}|c_k(\xi)|^2)^{(1/2)}]$.

Then, from Cauchy–Schwarz inequality, there follows:

$$\begin{aligned} E_\xi\left[\left(\sum_{k=0}^{\infty}|c_k(\xi)|^2\right)^{\frac{1}{2}}\right] &\le \left[E_\xi\left(\sum_{k=0}^{\infty}|c_k(\xi)|^2\right)\right]^{\frac{1}{2}}\big[E_\xi(1)\big]^{\frac{1}{2}} \\ &= \left[\sum_{k=0}^{\infty}E_\xi(|c_k(\xi)|^2)\right]^{\frac{1}{2}} \\ &= \|x\|_{\mathcal{N}} < \infty \end{aligned} \tag{8}$$

as assumed. Hence, $\sum_{k=0}^{\infty} E_\xi(c_k(\xi))z^k \in H^2(\mathbb{D})$.

Furthermore, the relation (7) holds because $c_k(\xi) = (1/2\pi)\int_0^{2\pi} x(e^{it},\xi)e^{-ikt}dt$ for each k is a continuous functional. ∎

For $\bar{x}$, according to (7), the n-best AFD approximation of $\bar{x}$ is

$$\tilde{\bar{x}}(z) = \sum_{k=1}^{n} c_k B_k \tag{9}$$

which best approximates $\bar{x}$ under a selection of the n-tuple of the parameters $\{a_k\}_{k=1}^n$. The learned n-TM system of $\bar{x}$ is $\{B_k\}_{k=1}^n$. We call the sparse coding vector of $\bar{x}$ with $\{B_k\}_{k=1}^n$ is the *functional representation* under the learned n-TM system $\{B_k\}_{k=1}^n$, which can be written as

$$c_k = \langle \bar{x}, B_k\rangle = \big\langle \bar{x}, B_{a_1,\ldots,a_k}\big\rangle. \tag{10}$$

The characteristic of SAFD is embedded in the parameter selection. An optimal selection of the parameters $a_1, a_2, \ldots, a_n$ is based on minimizing the square-distance between $\bar{x}$ and $\tilde{\bar{x}}$, that is,

$$\left|\left|\bar{x} - \sum_{k=1}^{n}\big\langle \bar{x}, B_{a_1,\ldots,a_k}\big\rangle B_{a_1,\ldots,a_k}\right|\right|$$

$$= \min_{\{b_1,\ldots,b_k\}\subset\mathbb{D}} \left\| \bar{x} - \sum_{k=1}^{n} \langle \bar{x}, B_{b_1,\ldots,b_k} \rangle B_{b_1,\ldots,b_k} \right\|. \quad (11)$$

The cyclic iteration process is used to solve the above optimization problem. That is, it adaptively selects one optimized parameter for each cycle based on the *maximal selection principle (MSP)* to reach the maximum energy [21], [22] and achieve fast convergence. Specifically, to achieve (11), we start from an initial value of the n-tuple parameter of $(b_1^{(0)}, \ldots, b_n^{(0)})$. Then we fix $b_2^{(0)}, \ldots, b_n^{(0)}$ and rename the $n-1$ points $(b_2^{(0)}, \ldots, b_n^{(0)})$ as $(d_1, \ldots, d_{n-1})$.

Set $\bar{x} = X_1$, then according to [21]

$$\bar{x}(z) = \sum_{k=1}^{n-1} \langle X_1, B_{\{d_1,\ldots,d_k\}} \rangle B_{\{d_1,\ldots,d_k\}} + X_n(z) \prod_{k=1}^{n-1} \frac{z - d_k}{1 - \bar{d}_k z} \quad (12)$$

where

$$X_n = \frac{X_{n-1} - \langle X_{n-1}, e_{d_1} \rangle e_{d_1}}{\frac{z - d_{n-1}}{1 - \bar{d}_{n-1} z}}. \quad (13)$$

X_n is the generalized backward shift of $X_{n-1}(z)$ through d_{n-1}.

By the reproducing kernel property of the evaluator, the inter product between X_n and e_b is [21]

$$\langle X_n, e_b \rangle = \sqrt{1 - |b|^2} X_n(b). \quad (14)$$

The MSP proved in [21] asserts that for X_n, there exists $b_1^{(1)} \in \mathbb{D}$ such that

$$b_1^{(1)} = \arg\max_{b\in\mathbb{D}} \left\{ \left(1 - |b|^2\right) |X_n(b)|^2 \right\}. \quad (15)$$

We then form a new n-tuple $(b_1^{(1)}, \ldots, b_n^{(1)})$. With these new parameters, we have the improvement of

$$\left\| \bar{x} - \sum_{k=1}^{n} \left\langle \bar{x}, B_{b_1^{(1)},\ldots,b_n^{(1)}} \right\rangle B_{b_1^{(1)},\ldots,b_n^{(1)}} \right\| < \left\| \bar{x} - \sum_{k=1}^{n} \left\langle \bar{x}, B_{b_1^{(0)},\ldots,b_n^{(0)}} \right\rangle B_{b_1^{(0)},\ldots,b_n^{(0)}} \right\|. \quad (16)$$

Repeating the same process to the time M such that none of the continuous n replacements of $b_k^{(M)}$ has a true improvement of $||\bar{x} - \sum_{k=1}^{n} \langle \bar{x}, B_{b_1^{(M)},\ldots,b_n^{(M)}} \rangle B_{b_1^{(M)},\ldots,b_n^{(M)}}||$. Then $(b_1^{(M)}, \ldots, b_n^{(M)})$ is the optimal parameters $(a_1, \ldots, a_n)$ that been finalized.

The iterative selection process of the parameters is also vividly shown in Fig. 1. As shown in Fig. 1, one more optimized parameter for each cycle is selected adaptively based on MSP to achieve the most representative atoms.

For $x(t, \xi)$, we have obtained a sequence of optimal parameters $\{a_k\}_{k=1}^n$ and an associated n-TM system $\{B_k\}_{k=1}^n$ that gives rise to the SAFD approximation $\tilde{x}(t, \xi)$ of $x(t, \xi)$, where

$$\tilde{x}(t, \xi) = \sum_{k=1}^{n} c_k(\xi) B_k \quad (17)$$

and $c_k(\xi) = \langle x(t, \xi), B_k \rangle$ is the functional representation of $x(t, \xi)$. According to (5), we have

$$\tilde{y}(t, \xi) = 2\mathcal{R}(\tilde{x}) - c_0 = 2\mathcal{R}\left(\sum_{k=1}^{n} \langle x(t, \xi), B_k \rangle B_k \right) - c_0 \quad (18)$$

where $\mathcal{R}$ means taking the real part.

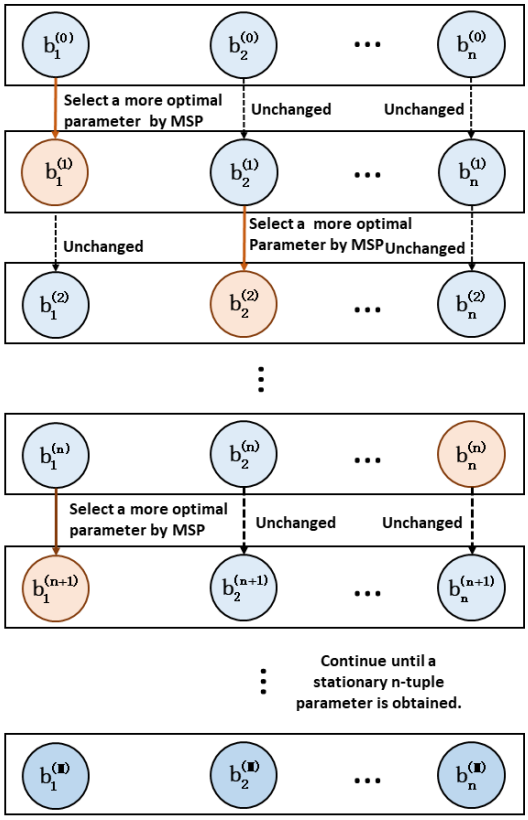

Fig. 1. Iterative selection process of parameters.

B. Effect of wBPs for ECG Signals

The ECG signal is based on the individualized mechanical movement of human heart, which contains the unique physiological information of the individual [3]. An ECG signal is composed of consecutive heartbeats. A complete heartbeat mainly includes P, QRS complex, and T wave [30]. It is reasonable that the heartbeats of the same subject should share similar characteristics, not only the waveform structure, but also the time–frequency characteristics. Moreover, due to the physiological diversity, these characteristics show different aspects for different subjects. Since the differences between subjects are relatively subtle, it is very challenging to visually distinguish these differences. In the proposed method, the n-TM system learned by SAFD contains the time–frequency characteristic of each heartbeat, which can effectively describe the inherent wave structure of the heartbeat. Through the improvement of the intra-subject compactness and the inter-subject dispersion by the learned n-TM system, we can extract effective features for personal identification.

A specific time–frequency representation of $x(t, \xi)$ is given by SAFD in (17), that is,

$$T_{x(t,\xi)}(t, \eta) = \sum_{k=1}^{n} \rho_k^2(t, \xi) \delta\left(\eta - \theta_k'(t)\right) \quad (19)$$

where $\eta > 0$ is the frequency and δ is the distributional Dirac function [31]

$$\rho_k(t, \xi) = |c_k(\xi)| \frac{\sqrt{1 - |a_k|^2}}{1 - |a_k| \cos(t - \theta_{a_k}) + |a_k|^2}$$

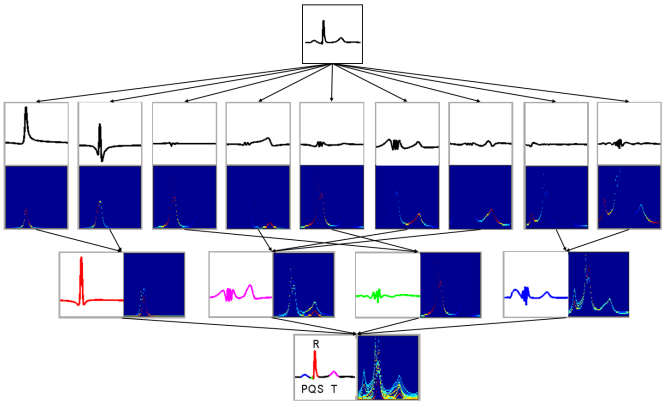

Fig. 2. wBPs and corresponding time–frequency representations of a heartbeat by SAFD.

is the instantaneous amplitude, and

$$\theta_k'(t) = \frac{|a_k|\cos(t-\theta_{a_k}) - |a_k|^2}{1 - 2|a_k|\cos(t-\theta_{a_k}) + |a_k|^2} + \sum_{j=1}^{k-1} \frac{1-|a_j|^2}{1-|a_j|\cos(t-\theta_{a_j}) + |a_j|^2}$$

is the instantaneous frequency, where $\theta_k = |a_k| e^{i\theta_{a_k}}$.

The time–frequency representation quantifies the time-varying properties of ECG signals. The morphology of the ECG signal evolves with time and space, so the time–frequency representation can reveal the joint temporal and spatial characteristics. For the purpose of visualization, all wBPs and their corresponding time–frequency representations of a heartbeat are illustrated in Fig. 2. In Fig. 2, the first row shows the original heartbeat and the last row shows the heartbeat of the SAFD approximation, along with its time–frequency representation calculated by (19). The second and third rows show each decomposed wBP and partial sums of selected wBP with their corresponding time–frequency representations, respectively. As shown in Fig. 2, each wBP plays a role in the composition of the wave, which corresponds to different wave components of P wave, QRS wave, and T wave. It can also be observed from the time–frequency representation that the spectral power of wBP is mainly concentrated in the frequency range of its related wave components.

To further demonstrate the effectiveness of the learned n-TM system, we use a visualization technique [32] to visualize the learned functional representations from (10) in Fig. 3. Fig. 3(a) and (b) shows two heartbeats with subtle change in wave morphology, selected randomly from two different subjects, respectively. Fig. 3(c) is the visualization of the two heartbeats embedded into two dimensions, while Fig. 3(d) is done in the same way on functional representations based on the learned n-TM system. It can be seen from the figure that although the heartbeats are so similar that it is difficult to distinguish them visually, the results after functional representation has become separable. It shows that the learned n-TM system is able to generate discriminative outputs.

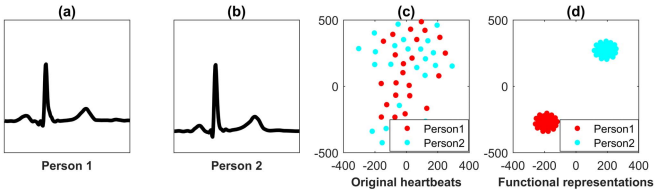

Fig. 3. Visualization of two heartbeats from two subjects. (a) and (b) Original heartbeats. (c) Original data points. (d) Result after the functional representations.

C. Proposed Sparse Representation Learning Framework

The framework of ECG biometric identification system is shown in Fig. 4. The method is implemented in three steps, including preprocessing, the sparse representation training, and matching process.

1) Preprocessing: Due to the practical demand for real-time identification, heartbeats, instead of long-term ECG records, are used in the proposed method. Therefore, ECG signals are mainly preprocessed by noise filtering, R location detection, and heartbeat segmentation [14]. ECG denoising and R-peak detection methods have been widely explored [33]–[35], which are beyond the scope of this study. A Butterworth bandpass filter is used to reduce noise for obtaining smoothed ECG signals, and the R-peak location is detected by the Elgendi algorithm [36]. In order to keep the complete information containing P, QRS complex, and T waves, as well as considering the heart rate variability, one-third durations of RR intervals before the R location and two-thirds durations thereafter is truncated as a heartbeat segmentation. Heart rate variability needs to be considered in the ECG biometric recognition, because it will affect the cycle length of the ECG signal, thereby affecting the accuracy of recognition [37]. The normalization step is usually used in other methods, which adjusts the heartbeat segments to a fixed length to reduce the influence of heart rate variability [14], [20]. In our method, all heartbeats are automatically mapped to the same period $[0, 2\pi)$ during the processing in SAFD. In this case, our method is not affected by heart rate variability, which is a superior advantage over other methods.

2) SAFD-Based Heartbeat Sparse Representation: Assume there are L subjects. The ith subject's training heartbeats are denoted as $S_i = (y_{i,1}, \ldots, y_{i,N_i})$, where N_i is the number of training heartbeats of the ith subject, $i = 1, \ldots, L$. Our goal is to learn a subject-specific n-TM system to represent the original training heartbeats S_i and obtain the sparse representation of S_i. First of all, the associated analytic signal of $y_{i,j}$ is $x_{i,j}$ that is calculated by (5), so $S_i^+ = (x_{i,1}, \ldots, x_{i,N_i})$. We write $x_{i,j}$ as $x_i(\xi_j)$, that is,

$$x_{i,j} = x_i(\xi_j), \quad j = 1, \ldots, N_i. \tag{20}$$

Then, according to (6)

$$x_i(\xi_j) = \bar{x}_i + r_i(\xi_j) \tag{21}$$

and $\bar{x}_i = E_\xi(x_i(\xi_j))$. $\bar{x}_i$ is as the template heartbeat of the ith subject.

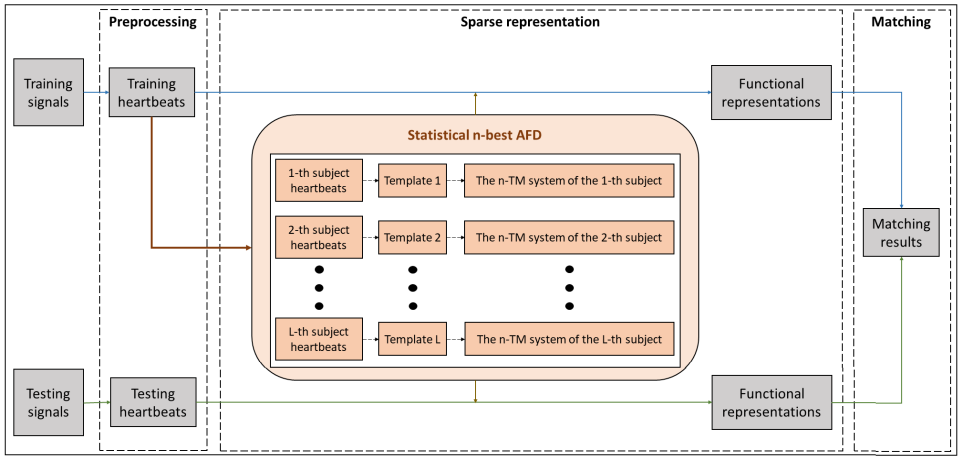

Fig. 4. Framework of the proposed SAFD for ECG biometric identification.

Algorithm 1 Parameter Selection Process of S_i^+

Input: $\bar{x}_i$, an initial value of the n-tuple parameter of $m_0 = (b_1^{(0)}, \ldots, b_n^{(0)})$.

Output: $(b_1^{(M)}, \ldots, b_n^{(M)})$.

1: Compute $\nabla E^{(M)} = \nabla E^{(0)} = ||\bar{x}_i - \sum_{k=1}^{n} \langle \bar{x}_i, B_{b_1^{(0)},\ldots,b_n^{(0)}} \rangle B_{b_1^{(0)},\ldots,b_n^{(0)}}||$, where M changes with the upper index value of ∇E.

2: Fix $b_2^{(0)}, \ldots, b_n^{(0)}$, rename the $n-1$ points as $(d_1, \ldots, d_{n-1})$;

3: Compute $\bar{x}_i - \sum_{k=1}^{n-1} \langle \bar{x}_i, B_{\{d_1,\ldots,d_k\}} \rangle B_{\{d_1,\ldots,d_k\}} = \bar{x}_{in} \prod_{k=1}^{n-1} \frac{z - d_k}{1 - \bar{d}_k z}$ by (12);

4: Use the MSP to $\bar{x}_{in}$, then get $b_1^{(1)} = \arg\max_{b \in \mathbb{D}} \{(1 - |b|^2)|\bar{x}_{in}(b)|^2\}$ by (15), $m_1 = (b_1^{(1)}, \ldots, b_n^{(1)})$ and $||\nabla E^{(1)}|| < ||\nabla E^{(0)}||$;

5: Keep $b_1^{(1)}$ and $b_3^{(1)}, \ldots, b_n^{(1)}$ unchanged in their positions, replace $b_2^{(1)}$ by $b_2^{(2)}$ in virtue of MSP to obtain the improvement of $||\nabla E^{(2)}|| < ||\nabla E^{(1)}||$;

6: Carry on this process to the time M such that none of the continuous n replacements of $b_k^{(M)}$ has a true improvement of $||\nabla E^{(M)}||$;

7: **return** $(b_1^{(M)}, \ldots, b_n^{(M)})$.

As described in Section II-A2, we need to select the optimal parameters $\{a_1^i, \ldots, a_n^i\}$ of $\bar{x}_i$ to constructed the n-TM system of S_i^+ such that

$$\left|\left|\bar{x}_i - \sum_{k=1}^{n} \left\langle \bar{x}_i, B_{a_1^i,\ldots,a_k^i} \right\rangle B_{a_1^i,\ldots,a_k^i}\right|\right| = \min_{\{b_1,\ldots,b_k\} \subset \mathbb{D}} \left|\left|\bar{x}_i - \sum_{k=1}^{n} \left\langle \bar{x}_i, B_{b_1,\ldots,b_k} \right\rangle B_{b_1,\ldots,b_k}\right|\right|. \quad (22)$$

The detailed parameter selection process is described in Algorithm 1 according to Section II-A2. The output $(b_1^{(M)}, \ldots, b_n^{(M)})$ in Algorithm 1 is as $\{a_1^i, \ldots, a_n^i\}$ of $\bar{x}_i$.

Then the corresponding wBPs of the ith subject's training heartbeats are acquired by (1), that is,

$$B_k^i(z) = B_{a_1^i,\ldots,a_k^i} = \frac{\sqrt{1 - |a_k^i|^2}}{1 - \bar{a}_k^i z} \prod_{j=1}^{k-1} \frac{z - a_j^i}{1 - \bar{a}_j^i z}. \quad (23)$$

$\{B_k^i\}_{k=1}^n$ is the learned n-TM system of S_i.

Now we have got the learned n-TM system of each subject's training heartbeats, namely $\{B_k^i\}_{k=1}^n$, $i = 1, \ldots, L$. Then the subject-specific n-TM system $\{B_k^i\}_{k=1}^n$ are combined as an unified n-TM system $\{B_1^1, \ldots, B_1^n, \ldots, B_L^1, \ldots, B_L^n\}$.

For $x_{i,j}$, the approximation $\tilde{x_{i,j}}$ of $x_{i,j}$, $j = 1, \ldots, N_i$ is obtained over the learned n-TM system $\{B_k^i\}_{k=1}^n$

$$\tilde{x_{i,j}} = \sum_{k=1}^{n} (c_{i,j})_k^i B_k^i \quad (24)$$

$(c_{i,j})_k^i = \langle x_{i,j}, B_k^i \rangle$ is the functional representation based on $\{B_k^i\}_{k=1}^n$. It can be seen from (23) and (24) that the functional representation $(c_{i,j})_k^i$ only uses the learned parameters $\{a_1^i, \ldots, a_n^i\}$. Furthermore, the unified functional representation of $x_{i,j}$ or $y_{i,j}$ can be obtained as $C_{i,j} = ((c_{i,j})_1^1, \ldots, (c_{i,j})_n^1, \ldots, (c_{i,j})_1^L, \ldots, (c_{i,j})_n^L)$.

Therefore, we get the unified functional representation C_i, $i = 1, \ldots, L$ of each subject' training heartbeats stored as templates for matching.

3) Matching: In the matching phase, to an unknown test heartbeat y of one subject, we need to find the best approximation of y and get the unified functional representation for final identification. The associated analytic signal of y is x, and the approximation $\tilde{x}^i$ are obtained over the learned n-TM system $\{B_k^i\}_{k=1}^n$, $i = 1, \ldots, L$, that is,

$$\tilde{x}^i = \sum_{k=1}^{n} c_k^i B_k^i \quad (25)$$

where c_k^i is the corresponding functional representation of $c_k^i = \langle x, B_k^i \rangle$. Hence, the unified functional representation of x or y is $C_x = (c_1^1, \ldots, c_n^1, c_1^2, \ldots, c_n^2, \ldots, c_1^L, \ldots, c_n^L)$.

TABLE I
CONFIGURATIONS OF ECG DATABASES

Databases	Sample rate	Records	Subjects	Age	Recording time	Health state
Fantasia	250Hz	40	40	21-85	2h	Health
MITDB	360 Hz	48	47	Not specified	30min	Health, Arrhythmia
ECG-ID	500Hz	310	90	13-75	20s	Unknown
EDB	250 Hz	90	79	30-84	2h	ST or T-wave changes
AED	1000 Hz	75	25	22-27	25min	Health

Finally, the test heartbeat y is determined as the hth subject whose distance is nearest

$$h = \arg \min_{i=1,\ldots,L} \|C_i - C_x\|_2^2. \tag{26}$$

In addition, the subject is identified as the hth subject, and the approximation of y is obtained by (17) and (18) as the following:

$$\tilde{y} = 2\mathcal{R}\left(\sum_{k=1}^{n} c_k^h B_k^h\right) - c_0. \tag{27}$$

D. Initial Parameters n and m_0 Settings

SAFD uses a fixed n to determine not only the size of the n-TM system $\{B_k\}_{k=1}^n$, but also the approximation accuracy. m_0 is the initial parameter value, which can affect the number of iterations and the calculation time of the algorithm. They can be set manually in advance and adjusted by the normalized residuals. Alternatively, they can be automatically estimated by applying the core AFD algorithm first [23]. In core AFD, the parameters $a_1, \ldots, a_k, \ldots$ are selected one by one automatically to construct an optimal sequence of wBPs to approximate the given signal. In this study, we use the core AFD to determine n and m_0.

E. Computation Complexity

The computation of SAFD is dominated by formula (5) and step 5 in Algorithm 1. Suppose the input ECG signal y is of length $N \in \mathbb{N}$. The computational complexity of (5) for getting the associated analytic signal is $\mathcal{O}(N)$ [25]. For the parameters selection process in Algorithm 1, a more optimized parameter is obtained in each cycle by the MSP of step 4. To implement the MSP, the computational complexity is $\mathcal{O}(CN \log N)$ as provided in [38], where C is the number of discrete points in $\mathbb{D}$ that is divided into rectangular grid for searching the maximum value to satisfy $b_1^{(j)} = \arg\max_{b\in\mathbb{D}}\{(1 - |b|^2)|\bar{x}_{in}(b)|^2\}$, where $j = 1, 2, \ldots, M$ is the number of iterations, and $i = 1, 2, \ldots, L$ is the number of subject. Therefore, in summary, the computational complexity of SAFD is $\mathcal{O}(N \log N)$ since C is determined. In practice, because each heartbeat is fixed and short, the calculating time is expected to be small.

III. EXPERIMENTAL RESULTS

The principle of our method is to learn a heartbeat sparse representation for each subject. Then, for any given ECG signal, our method recognizes which subject the heartbeat belongs to according to its sparse representation, thereby realizing ECG-based biometric identification. Recognition can be achieved by matching single or multiple heartbeats. In this section, the ECG databases and initial parameter settings used in this study are briefly introduced first. Then, the performance evaluation metrics are provided. Finally, the comprehensive evaluations of our method on five ECG databases are presented in three aspects, including single and multiple heartbeats recognition, and comparison experiments.

A. ECG Databases and Initial Parameter Settings

The proposed SAFD is evaluated on four widely used public databases, including Fantasia database (Fantasia),[1] MIT-BIH arrhythmia database (MITDB),[2] ECG-ID database (ECG-ID),[3] and European ST-T database (EDB).[4] The data in these databases are collected under different sample rates, number of records and subjects, recording time, age, and health status. To further evaluate the method, one more database, Aveiro ECG database (AED) [39], [40], is used, which data were collected through three different sessions, apart from each other for one week. The detailed information of these databases is listed in Table I.

We divided the heartbeats into two groups, that is, training and test heartbeats. The test heartbeats can be further divided into two categories, including same time interval and cross time interval heartbeats. The same time interval heartbeats mean that the training data and test data come from the ECG signals with a short time interval, for example, consecutive heartbeats immediately after the training heartbeats or the heartbeats that are only a few seconds apart from the training heartbeats. The cross time interval heartbeats mean that the training data and the test data come from different time periods, such as different hours, even different days. The former has smaller changes between training and testing heartbeats, while the latter has larger changes. Taking into account the real situation of personal identification, the cross time interval test is more realistic. In this aspect, AED conforms to the ECG signal used for biometric identification in practice. The time interval of the other four public databases is not labeled clearly. To compare with other studies, two different kinds of experiments were conducted on each database, that is, same time interval and cross time interval experiments. We try to take the heartbeats that are far apart for training and testing as the cross time interval experiments.

[1] https://physionet.org/content/fantasia
[2] https://physionet.org/content/mitdb
[3] https://physionet.org/content/ecgiddb
[4] https://physionet.org/content/edb

TABLE II
PARAMETERS AND IDENTIFICATION PERFORMANCE OF THE PROPOSED METHOD ON FIVE DATABASES

Database	m_0	n	Cross time interval mode		
			Se	Spe	RAC
Fantasia	(-0.8-0.2i,0.5,-0.9-0.2i,0.1-0.5i,-0.3+0.4i,0.1+0.3i -0.6-0.2i,0.5+0.7i,0.5i,-0.4+0.6i,-0.2-0.7i,-0.1i)	12	0.9946	0.9945	99.46
MITDB(25)	(0.7-0.4i,0.9i,-0.1-0.7i,0.8-0.1i,-0.7+0.6i,-0.5-0.6i 0.1-0.5i,0.3-0.5i,0.7+0.5i,0.4+0.6i,0.6+0.7i,-0.1+0.6i)	12	0.9985	0.9985	99.85
MITDB(47)	(-0.5+0.7i,0.7-0.2i,-0.5+0.6i,-0.2+0.7i,-0.3+0.5i,0.9 0.5+0.5i,-0.6i,-0.7+0.6i,-0.1+0.4i,-0.2-0.4i,-0.5+0.8i)	12	0.9824	0.9825	98.25
ECG-ID	(-0.1+0.9i,0.6-0.3i,-0.6+0.6i,0.4+0.2i,-0.3-0.2i,0.1+0.5i -0.5+0.5i,-0.3,0.7,0.4-0.8i,0.8+0.1i,0.3-0.2i)	12	0.9789	0.9789	97.89
EDB(20)	(-0.6+0.3i,0.5+0.4i,-0.9+0.1i,0.7+0.5i,-0.3-0.8i,-0.4+0.3i 0.8-0.3i,-0.3+0.5i,0.2+0.4i,0.8+0.1i,0.5-0.7i,0.4-0.4i)	12	0.9610	0.9610	96.13
EDB(40)	(-0.4+0.5i,0.2-0.6i,0.2+0.1i,0.1-0.3i,-0.3i,0.3-0.8i 0.3+0.3i,0.6+0.7i,-0.4-0.2i,-0.8+0.4i,0.5+0.8i,0.1-0.5i)	12	0.9171	0.9170	96.55
EDB(60)	(-0.2+0.3i,-0.3+0.1i,0.2+0.8i,0.4-0.7i,-0.7+0.2i,0.6+0.1i 0.4+0.3i,0.3-0.7i,-0.4+0.7i,0.6,-0.4-0.2i,-0.8-0.5i)	12	0.8965	0.8965	94.83
EDB(79)	(-0.7+0.4i,-0.1+0.6i,-0.5+0.3i,0.8-0.1i,-0.7-0.6i,0.3i -0.8-0.5i,0.7+0.1i,-0.8-0.2i,-0.3+0.5i,0.3+0.6i,-0.9-0.1i)	12	0.9367	0.9374	93.74
AED	(-0.2-0.1i,-0.3+0.4i,-0.7+0.5i,0.6-0.3i,0.1+0.6i,0.4 0.4-0.7i,-0.7-0.3i,-0.4-0.2i,0.7+0.6i,0.3-0.9i,-0.6+0.6i)	12	0.9996	0.9996	99.90

There are two parameters to be set, that is, n and m_0. By applying the core AFD algorithm, $n = 12$ is obtained as the initial n of SAFD. $m_0 = (b_1^{(0)}, \ldots, b_{12}^{(0)})$ is the parameters obtained by the core AFD algorithm with $n = 12$. The detailed parameter values of each database are presented in Table II.

B. Performance Evaluation Metrics

The recognition performance of the proposed method is evaluated by the recognition accuracy (RAC) and the confusion matrix. The RAC is the ratio of the number of correctly identified subjects to the number of all subjects, which is defined as [39]

$$\text{RAC} = \frac{\text{TP} + \text{TN}}{\text{TP} + \text{FP} + \text{TN} + \text{FN}} \tag{28}$$

where TP is the number of true positives, TN is the number of true negatives, FP is the number of false positives, and FN is the number of false negatives. The sensitivity (Se) represents the ability of an identification system to identify someone correctly and the specificity (Spe) evaluates the ability of the identification system to reject someone correctly, and they are as follows [39]:

$$\text{Se} = \frac{\text{TP}}{\text{TP} + \text{FN}} \tag{29}$$

$$\text{Spe} = \frac{\text{TN}}{\text{FP} + \text{TN}}. \tag{30}$$

The confusion matrix provides a detailed distribution of the recognition performance of each subject. Assume there are L subjects, then the confusion matrix is an L square matrix.

Furthermore, the verification performance is evaluated using equal error rate (EER) [20]. EER is a point on the detection error tradeoff curve where the false acceptance rate (FAR) equals the false rejection rate (FRR). FAR is the probability that two non-mate samples will be incorrectly recognized as a match, while FRR refers to the probability that two mate samples will be falsely declared as non-match. A varied threshold for using to verify the authenticity of the test sample is used to yield a plot of FAR, FRR, and EER. Here, lower EER means better identification system.

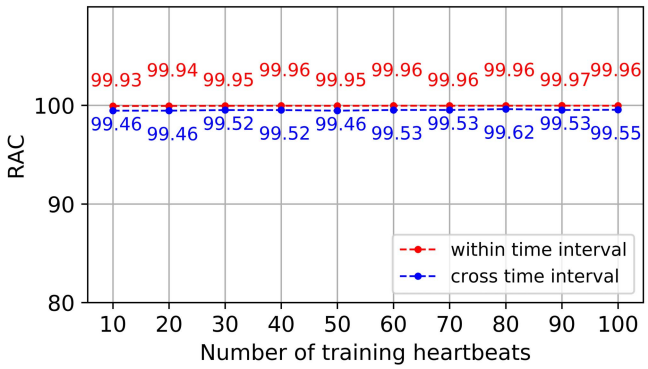

Fig. 5. Comparison of the RAC of different numbers of training heartbeats on Fantasia.

C. ECG Biometric Identification by Matching Single Heartbeat

1) Experimental Results on Fantasia: Unlike most other databases in PhysioNet, ECG signals of the Fantasia database are all from healthy subjects with similar signal waveforms. The first 10, 20, 30, 40, 50, 60, 70, 80, 90, and 100 heartbeats of each subject are used as the training heartbeats. The detailed RAC of different number of training samples is plotted in Fig. 5. As shown in Fig. 5, the minimum of RAC is 99.93% and the maximum of RAC is 99.97% in the same time interval mode; the RACs in the cross time interval mode are from 99.45% to 99.62%. It is reasonable that the performance of the same time interval mode is better than that of the cross time interval mode. It can be seen from Fig. 5 that the performance of different number of training heartbeats does not change

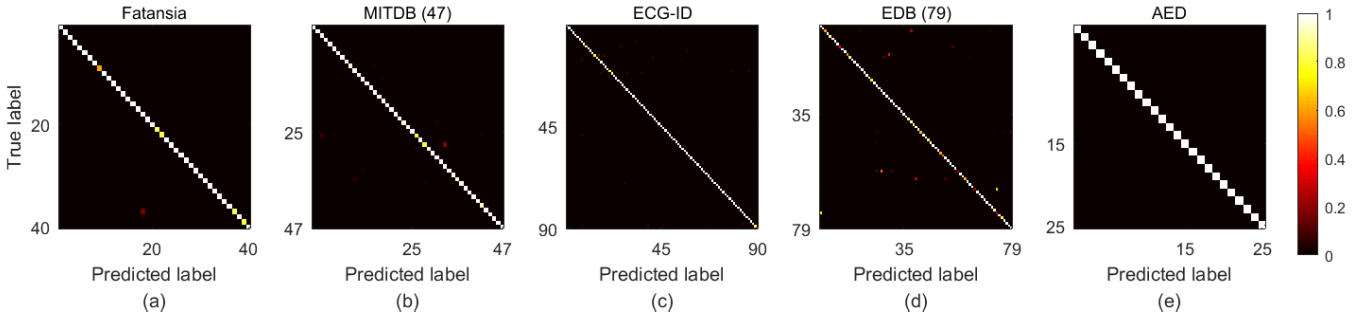

Fig. 6. Confusion matrix for identification performance on the test databases listed in Table II with the cross time interval mode. (a) Confusion matrix of Fatansia. (b) Confusion matrix of MITDB. (c) Confusion matrix of ECG-ID. (d) Confusion matrix of EDB. (e) Confusion matrix of AED.

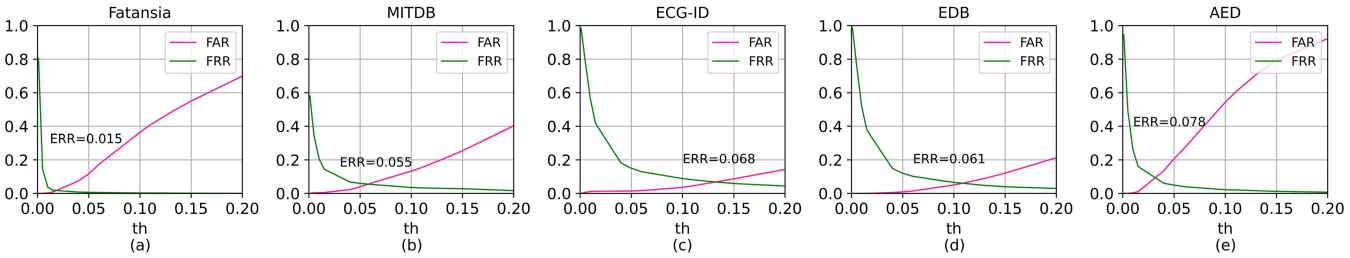

Fig. 7. FAR-FRR curves of the test databases listed in Table II with the cross time interval mode. (a) FAR-FRR curve of Fatansia. (b) FAR-FRR curve of MITDB. (c) FAR-FRR curve of ECG-ID. (d) FAR-FRR curve of EDB. (e) FAR-FRR curve of AED. The threshold is abbreviated as th that is varied to yield the plot of FAR-FRR curve.

much. Therefore, considering the calculation cost and storage space, in the subsequent experiments, we set ten heartbeats as the training number.

Table II presents the Se of 99.46%, Spe of 99.45%, and RAC of 99.46% on the test heartbeats in the cross time interval mode and Fig. 6(a) shows the corresponding confusion matrix. Heartbeats not shown on the diagonal of the confusion matrix are false matches. It can be seen that the test heartbeats are almost on the diagonal, which shows that the proposed method achieves a higher recognition rate on the Fantasia database. The test performance of the FAR and FRR of the Fantasia database in the cross time interval mode is shown in Fig. 7(a). The EER is 0.015 as shown in Fig. 7(a), which proves that the proposed method is an effective identification system.

2) Experimental Results on MITDB: The MIT-BIH arrhythmia database is widely used in various methods [6], [8], [12], [13], [20], [41]. However, this database is mainly to record the data on different arrhythmia heart diseases. Therefore, we conduct experiments on this database by using 25 records of relatively wave shape control subjects and all 48 records of 47 subjects separately. In the same time interval mode, the RAC of identifying 25 subjects reaches 99.95% and identifying 47 subjects reaches 99.46%. The results in the cross time interval mode are list in Table II. For identifying 47 subjects of MITDB, the RAC of the cross time interval mode is 98.25%. The confusion matrix and the FAR and FRR curves of the cross time interval mode for testing 47 subjects' data are presented in Figs. 6(b) and 7(b), respectively.

3) Experimental Results on ECG-ID: Each record in the ECG-ID database is about 20 s, so the number of heartbeats obtained from each record is not much. There are several records for each subject, and therefore, we only perform the cross interval experiments on this database. Specifically, for each subject, training heartbeats are taken from one record and test heartbeats are taken from another record. The RAC of the ECG-ID database is 97.89% as shown Table II and the confusion matrix is presented in Fig. 6(c). Besides, the FAR, FRR, and EER of the ECG-ID database are displayed in Fig. 7(c).

4) Experimental Results on EDB: EDB contains a large number of subjects whose ECG records are with long periods of time and is suitable for evaluating the impact of database scales or the number of subjects on the proposed method. Hence, we test performance for different database scales based on this database. When the test data come from 20, 40, 60, and all subjects' data, RAC achieves 99.83%, 99.75%, 99.68%, and 99.55% in the same time interval mode, and 96.13%, 96.55%, 94.83%, and 93.74% in the cross time interval mode, respectively. The results of the cross time interval mode in terms of different database scales are list in Table II. The confusion matrix of the test data from all subjects' data in the cross time interval mode are shown in Fig. 6(d) and the FAR and FRR curves are shown in Fig. 7(d). It can be seen in Fig. 6(d) that there are a few false matching samples in the confusion matrix for larger scales, but the RACs are still high. Furthermore, this database records diseases related to ST and T wave changes, not normal signals, which is an indication that the proposed method is useful and reproducible in real contexts.

5) Experimental Results on AED: Most public databases are used for clinical analysis and monitoring of certain heart diseases, and personal identification is not taken into account. AED is specifically designed for the purpose of personal

TABLE III

PERFORMANCE COMPARISON BETWEEN THE PROPOSED METHOD AND [39] ON AED

Methods	Database	Algorithm	Time Duration	Acc(%)
S. Brás et al. [39]	AED	compression algorithm	1.5min	98.03
SAFD	AED	SAFD	1s	**99.93**

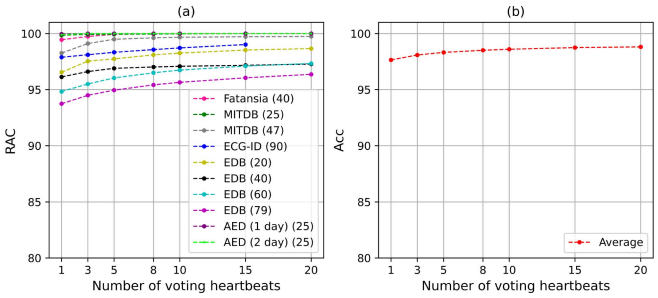

Fig. 8. RAC of varying vote heartbeats on test databases. (a) RAC of each test database. (b) Average RAC of five databases.

biometric and emotion identification. It is very suitable for evaluating the robustness of the proposed method, which is independent of the signals collected at different hours, days, and human emotions. In this database, the heartbeats of ECG signals collected on the first day are used for training, and the data collected on the other days are used for testing. The identification results are listed in Tables II and III. The corresponding confusion matrix and the FAR and FRR curves of the cross time interval mode are shown in Figs. 6(e) and 7(e), respectively. As shown in Table II, the RAC is 99.90%. The results show that the proposed method can achieve a remarkable performance in a dedicated biometric database, even in which ECG data collected from different realistic conditions, such as hours, days, and human emotions. Therefore, the proposed method is somehow immune to variability induced by different data collection sessions.

D. ECG Biometric Identification by Matching Multiple Heartbeats

Considering the security of identity recognition, in order to improve the reliability and recognition performance, it is usually adopted to recognize multiple consecutive heartbeats, known as the voting heartbeat method [6], [14]. Voting experiments with 1, 3, 5, 8, 10, 15, and 20 heartbeats are conducted. Since the test heartbeats of some subjects in ECG-ID are less than 20, the voting experiment on 20 was not carried out in it. The identification results on the five databases under the cross time interval mode are shown in Fig. 8.

It can be seen in Fig. 8(b), if only one heartbeat used for identification, the average accuracy (Acc) of five databases is 97.59%. It demonstrates that the proposed method has a good ability for identification by single heartbeat. If three heartbeats are used, the identification accuracy of AED can reach 100%. In addition, when the heartbeat vote is 15, the RAC of Fantasia and MITDB are both 100%. In practical applications, the balance between the RAC, the acquisition time, and the computational complexity needs to be considered. For real-time implementation in practice, in this study, we use three heartbeats for final recognition with an average RAC of 98.0%.

E. Performance Comparisons

Although personal identification based on ECG signals has been explored for more than ten years, there is still no standard criterion for comparing the performance of different methods. The main reason is that the databases used are inconsistent. For example, different methods use different public databases, or some methods only use part of the data in the same database, and some methods use private databases. In our method, we use all data from five databases, that is, Fatansia, MITDB, ECG-ID, EDB, and AED. In order to make a fair comparison with other state-of-the-art methods, in this study, we use the following items for comparison, including the number and scale of databases used, the main algorithms used for identification, the types of the feature extraction methods, the mathematical interpretability of the extracted features, the duration of the ECG signal used for one recognition, and the corresponding Acc. Our proposed methods is compared with the other 12 state-of-the-art methods, where the comparison results with the other 11 methods on public databases are shown in Table IV and the comparison results with the other one method on AED database are shown in Table III.

In Table IV, it can be seen the number and scale of databases used by each method are different. Among 12 comparison methods (including 11 state-of-the-art methods and the proposed method), the methods used in [10], [13], [14], [19], and [43] and the proposed method are verified on multiple databases. The other methods are only tested on one database. Except for the ECG database collected privately by themselves in [11], the ECG signals of other methods are all from online public databases. Besides, [8], [12], [13], [18], [19], [42], and [43] selected part of data in the database to conduct experiments. The proposed method is evaluated on both the public databases (Table IV) and the database collected under different realistic conditions (Table III). In Table IV, there are four learning-based methods, where the proposed method is the only one that can be described mathematically. The Acc of using 3 and 10 s ECG signal for once identification of the proposed method is 98.1% and 98.6%, respectively. Compared with other methods with the same time duration, the proposed method is most accurate. Brás *et al.* [39] in Table III used AED to verify their method and achieved Acc of 98.03%. 99.93% Acc of the proposed method by using the same database outperforms that of [39] as shown in Table III.

In addition, several prominent methods only use the MIT-BIH arrhythmia database and the ECG-ID database and just provide their respective accuracy rather than the average recognition rate, so a comparison of the proposed method against these methods with these two databases is provided in Table V. As shown in Table V, when we use three heartbeats for the identification, the RAC on the MITDB database and the ECG-ID database is 99.10% and 98.11%, respectively. Compared with the same number of heartbeats used in [6] and [20], our method is more accurate on the

TABLE IV
PERFORMANCE COMPARISON WITH OTHER METHODS

Methods	Database		Algorithm	Feature		Time Duration	Acc(%)
	Number	Scale		Type	Mathematical interpretability		
A. Pal and Y. Singh. [42]	1	100 subjects	Haar WT	manual	No	30s	97.12
Q. Zhang et al. [10]	8	18-47 subjects	WT, CNN	learned	No	2s	93.5
A. Chan et al. [11]	1	50 subjects	wavelet distance measure	manual	No	1s	89.0
X. Tang and L. Shu [12]	1	10 subjects	WT, RS-QNN	manual	Yes	1s	91.7
C. Ye et al. [13]	3	18-65 subjects	WT	manual	Yes	1s	85.5
Z. Zhao et al. [43]	3	25-90 subjects	EMD	manual	No	5s / 10s	82.2 / 95.6
H. Jaafar et al. [18]	1	79 subjects	autocorrelation, KSRC	manual	No	1s	97.23 / 95.87
Y. Li et al. [14]	5	18-40 subjects	CNN	learned	No	3s / 10s	94.3 / 97.1
Y. Huang et al. [19]	2	63-64 subjects	sparse representation	learned	No	1s	87.75 / 97.38
C. Ting and S. Salleh [8]	1	13 subjects	EKF	manual	No	30s	87.5
V. Mai et al. [15]	1	18 subjects	MLP, RBF-NN	manual	No	1s	98.0
Proposed	5	20-90 subjects	SAFD	learned	Yes	3s /10s	**98.1 / 98.6**

TABLE V
PERFORMANCE COMPARISON ON MITDB AND ECG-ID

Methods	Number of heartbeats	Database	
		MITDB	ECG-ID
Z. Zhao et al. [5]	–	–	96.63
R. Li et al. [6]	3	100	98.03
D. Rezgui and Z. Lachiri [41]	–	98.8	–
J. Wu and Y. Zhang [45]	–	99.64	–
J. Xu et al. [20]	3	100	93.26
Y. Chu et al. [44]	–	95.99	98.24
Proposed	3	99.10	98.11

TABLE VI
COMPARISON OF THE COMPUTATION TIME BETWEEN THE PROPOSED METHOD AND OTHER METHODS

Methods	Database	Training time/ Feature extraction time (s)	Matching time (s)
Z. Zhao et al. [5]	ECG-ID	5.2094	1.042
R. Li et al. [6]	ECG-ID	0.3316	0.008
	MITDB	0.0914	0.007
Y. Li et al. [14]	Fatansia	2400	2
Proposed	ECG-ID	1.2728	0.00075
	MITDB	0.4927	0.00068
	Fatansia	0.2898	0.0005

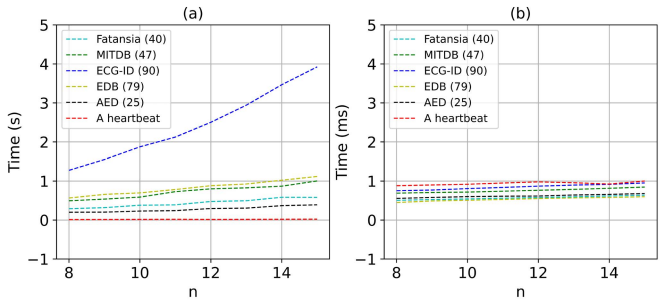

Fig. 9. Computation time. (a) Computation time of SAFD with different n, where n is the parameter of the learned n-TM system. (b) Computation time of the corresponding matching time.

ECG-ID database. Due to the use of all data of the MITDB database, the RAC of MITDB is not the best, but it is also comparable to [6] and [20], which removed heartbeats that are shaped changed heavily or abnormal. Furthermore, using the highest performance of our method compared with other methods in Table V, the RAC on the MITDB database is 99.74% and on the ECG-ID database is 99.02% as shown in Fig. 8, which is better than [44] of 95.99% and 98.24%, respectively. As it can be seen in Tables III–V, the proposed method achieves best performance compared with the other state-of-the-art methods.

F. Real-Time Implementation

All experiments in this study are performed on a computer with 16 GB of RAM and a 2.71 GHz Intel Core i5 processor. Note that there is no acceleration technology used to increase the speed, such as CNN in [10] and [14] for parallel computing. The main algorithm is developed in MATLAB R2016a.

The time of the sparse representation of heartbeats based on SAFD and the matching time are calculated. The critical part of sparse representation is to construct the learned n-TM systems. The calculation time required for each database to complete a training process to learn n-TM systems with different n is shown in Fig. 9(a). The training time depends on the number of subjects in the database. For Fatansia and ECG-ID with 40 and 79 subjects, respectively, the training times are below 1 s. For ECG-ID with 90 subjects, the training time is about 4 s on $n = 14$. As the training time in the learning method, it is already short enough. After the learned n-TM systems are established, the matching time will be fast. The average matching time is reported in Fig. 9(b), where the times are less than 1 ms for all databases. It demonstrates the potential for real-time implementation in practical application scenarios. As few methods provide the computation time, a comparison with selected methods that illustrate the algorithm time is presented in Table VI. As it can be observed in Table VI, the proposed method is more advantageous in terms of training time and matching time, which further suggests that it can serve as an effective real-time method for ECG biometric identification.

IV. CONCLUSION AND FUTURE WORKS

This article proposed a new sparse representation learning framework SAFD for ECG biometric identification. It can improve the intra-class compactness and inter-class dispersion of extracted features. It achieves a final robust and discriminative representation by the learned n-TM system, which reflect

the wave structure with time–frequency distribution of ECG signals. Experimental results demonstrate the effectiveness and efficiency of the proposed method for personal identification. The limitation of the system is that it needs some preprocessing operations. In addition, the recognition ability is reduced for the people with large heartbeat changes caused by heart disease that may change the time–frequency of the heartbeat itself. In future work, we will focus on reducing preprocessing operations and explore more robust features of ECG signals containing more uncontrolled conditions (especially pathological properties) to develop a broad identification system suitable for any external conditions. Furthermore, we will also explore the application of the proposed method to other physiological traits to develop other types of biometric identification systems.

REFERENCES

[1] A. K. Jain, A. A. Ross, and K. Nandakumar, *Introduction to Biometrics*. Springer, 2011.

[2] J. A. Unar, W. C. Seng, and A. Abbasi, "A review of biometric technology along with trends and prospects," *Pattern Recognit.*, vol. 47, no. 8, pp. 2673–2688, 2014.

[3] A. A. Alariki, "A review study of heartbeat biometric authentication," *J. Comput.*, vol. 13, no. 8, pp. 936–947, 2018.

[4] L. Biel, O. Pettersson, L. Philipson, and P. Wide, "ECG analysis: A new approach in human identification," *IEEE Trans. Instrum. Meas.*, vol. 50, no. 3, pp. 808–812, Jun. 2001.

[5] Z. Zhao, Y. Zhang, Y. Deng, and X. Zhang, "ECG authentication system design incorporating a convolutional neural network and generalized S-transformation," *Comput. Biol. Med.*, vol. 102, pp. 168–179, Nov. 2018.

[6] R. Li, G. Yang, K. Wang, Y. Huang, F. Yuan, and Y. Yin, "Robust ECG biometrics using GNMF and sparse representation," *Pattern Recognit. Lett.*, vol. 129, pp. 70–76, Jan. 2020.

[7] S.-C. Wu, P.-T. Chen, A. L. Swindlehurst, and P.-L. Hung, "Cancelable biometric recognition with ECGs: Subspace-based approaches," *IEEE Trans. Inf. Forensics Security*, vol. 14, no. 5, pp. 1323–1336, May 2019.

[8] C.-M. Ting and S.-H. Salleh, "ECG based personal identification using extended Kalman filter," in *Proc. 10th Int. Conf. Inf. Sci., Signal Process. Appl. (ISSPA)*, May 2010, pp. 774–777.

[9] A. Fratini, M. Sansone, P. Bifulco, and M. Cesarelli, "Individual identification via electrocardiogram analysis," *Biomed. Eng. Online*, vol. 14, no. 1, p. 78, 2015.

[10] Q. Zhang, D. Zhou, and X. Zeng, "HeartID: A multiresolution convolutional neural network for ECG-based biometric human identification in smart health applications," *IEEE Access*, vol. 5, pp. 11805–11816, 2017.

[11] A. D. C. Chan, M. M. Hamdy, A. Badre, and V. Badee, "Wavelet distance measure for person identification using electrocardiograms," *IEEE Trans. Instrum. Meas.*, vol. 57, no. 2, pp. 248–253, Feb. 2008.

[12] X. Tang and L. Shu, "Classification of electrocardiogram signals with RS and quantum neural networks," *Int. J. Multimedia Ubiquitous Eng.*, vol. 9, no. 2, pp. 363–372, 2014.

[13] C. Ye, M. T. Coimbra, and B. V. K. V. Kumar, "Investigation of human identification using two-lead Electrocardiogram (ECG) signals," in *Proc. 4th IEEE Int. Conf. Biometrics, Theory, Appl. Syst. (BTAS)*, Sep. 2010, pp. 1–8.

[14] Y. Li, Y. Pang, K. Wang, and X. Li, "Toward improving ECG biometric identification using cascades convolutional neural networks," *Neurocomputing*, vol. 391, pp. 83–95, May 2020.

[15] V. Mai, I. Khalil, and C. Meli, "ECG biometric using multilayer perceptron and radial basis function neural networks," in *Proc. Annu. Int. Conf. IEEE Eng. Med. Biol. Soc. (EMBC)*, Aug. 2011, pp. 2745–2748.

[16] R. D. Labati, E. Muñoz, V. Piuri, R. Sassi, and F. Scotti, "Deep-ECG: Convolution neural networks for ECG biometric recognition," *Pattern Recognit. Lett.*, vol. 126, pp. 78–85, Sep. 2019.

[17] J. Wang, M. She, S. Nahavandi, and A. Kouzani, "Human identification from ECG signals via sparse representation of local segments," *IEEE Signal Process. Lett.*, vol. 20, no. 10, pp. 937–940, Oct. 2013.

[18] H. Jaafar, N. H. Ramli, and A. S. A. Nasir, "Implementation of kernel sparse representation classifier for ECG biometric system," *J. Telecommun., Electron. Comput. Eng.*, vol. 10, pp. 89–94, May 2018.

[19] Y. Huang, G. Yang, K. Wang, H. Liu, and Y. Yin, "Learning joint and specific patterns: A unified sparse representation for off-the-person ECG biometric recognition," *IEEE Trans. Inf. Forensics Security*, vol. 16, pp. 147–160, 2020.

[20] J. Xu, G. Yang, K. Wang, Y. Huang, H. Liu, and Y. Yin, "Structural sparse representation with class-specific dictionary for ECG biometric recognition," *Pattern Recognit. Lett.*, vol. 135, pp. 44–49, Jul. 2020.

[21] T. Qian and Y. B. Wang, "Adaptive decomposition into basic signals of nonnegative instantaneous frequencies—A variation and realization of greedy algorithm," *Adv. Comput. Math.*, vol. 34, no. 3, pp. 279–293, 2010.

[22] T. Qian, "Cyclic AFD algorithm for the best rational approximation," *Math. Methods Appl. Sci.*, vol. 37, no. 6, pp. 846–859, 2014.

[23] T. Qian, L. Zhang, and Z. Li, "Algorithm of adaptive Fourier decomposition," *IEEE Trans. Signal Process*, vol. 59, no. 12, pp. 5899–5906, Dec. 2011.

[24] J. Ma, T. Zhang, and M. Dong, "A novel ECG data compression method using adaptive Fourier decomposition with security guarantee in e-health applications," *IEEE J. Biomed. Health Inform.*, vol. 19, no. 3, pp. 986–994, May 2015.

[25] C. Tan, L. Zhang, and H.-T. Wu, "A novel Blaschke unwinding adaptive-Fourier-decomposition-based signal compression algorithm with application on ECG signals," *IEEE J. Biomed. Health Inform.*, vol. 23, no. 2, pp. 672–682, Mar. 2019.

[26] X. Wang, T. Qian, I. Leong, and Y. Gao, "Two-dimensional frequency-domain system identification," *IEEE Trans. Autom. Control*, vol. 65, no. 2, pp. 577–590, Feb. 2020.

[27] Y. Li, L. Zhang, and T. Qian, "2D partial unwinding—A novel nonlinear phase decomposition of images," *IEEE Trans. Image Process.*, vol. 28, no. 10, pp. 4762–4773, Oct. 2019.

[28] T. Qian, "A sparse representation of random signals," 2020, *arXiv:2008.10473*. [Online]. Available: http://arxiv.org/abs/2008.10473

[29] C. Tan, L. Zhang, and T. Qian, "A new supervised learning approach: Statistical adaptive Fourier decomposition (SAFD)," in *Proc. Int. Conf. Neural Inf. Process.* Cham, Switzerland: Springer, 2019, pp. 397–404.

[30] L. Ivanciu, P. Farago, and S. Hintea, "A review of ECG based biometric systems," *Acta Tech. Napocensis*, vol. 59, no. 4, pp. 1–4, 2018.

[31] L. Zhang, T. Qian, W. Mai, and P. Dang, "Adaptive Fourier decomposition-based dirac type time-frequency distribution," *Math. Methods Appl. Sci.*, vol. 40, no. 8, pp. 2815–2833, May 2017.

[32] L. van der Maaten and G. Hinton, "Visualizing data using t-SNE," *J. Mach. Learn. Res.*, vol. 9, pp. 2579–2605, Nov. 2008.

[33] E. J. D. S. Luz, W. R. Schwartz, G. Cámara-Chávez, and D. Menotti, "ECG-based heartbeat classification for arrhythmia detection: A survey," *Comput. Methods Programs Biomed.*, vol. 127, pp. 144–164, Apr. 2016.

[34] R. Sameni, M. B. Shamsollahi, C. Jutten, and G. D. Clifford, "A nonlinear Bayesian filtering framework for ECG denoising," *IEEE Trans. Biomed. Eng.*, vol. 54, no. 12, pp. 2172–2185, Dec. 2007.

[35] J. Pan and W. J. Tompkins, "A real-time QRS detection algorithm," *IEEE Trans. Biomed. Eng.*, vol. BME-3, no. 3, pp. 230–236, Mar. 1985.

[36] M. Elgendi, "Fast QRS detection with an optimized knowledge-based method: Evaluation on 11 standard ECG databases," *PLoS ONE*, vol. 8, no. 9, Sep. 2013, Art. no. e73557.

[37] S. Pathoumvanh, S. Airphaiboon, and K. Hamamoto, "Robustness study of ECG biometric identification in heart rate variability conditions," *IEEJ Trans. Electr. Electron. Eng.*, vol. 9, no. 3, pp. 294–301, May 2014.

[38] Y. Gao, M. Ku, T. Qian, and J. Wang, "FFT formulations of adaptive Fourier decomposition," *J. Comput. Appl. Math.*, vol. 324, pp. 204–215, Nov. 2017.

[39] S. Brás *et al.*, "Biometric and emotion identification: An ECG compression based method," *Frontiers Psychol.*, vol. 9, p. 467, Apr. 2018.

[40] J. M. Carvalho, S. Brás, and A. J. Pinho, "Compression-based classification of ECG using first-order derivatives," in *Proc. Int. Conf. Intell. Technol. Interact. Entertainment (INTETAIN)*, vol. 273. Cham, Switzerland: Springer, 2018, pp. 27–36.

[41] D. Rezgui and Z. Lachiri, "ECG biometric recognition using SVM-based approach," *IEEJ Trans. Electr. Electron. Eng.*, vol. 11, no. 1, pp. S94–S100, Jun. 2016.

[42] A. Pal and Y. N. Singh, "ECG biometric recognition," in *Proc. Int. Conf. Math. Comput.* Cham, Switzerland: Springer, 2018, pp. 61–73.

[43] Z. Zhao, L. Yang, D. Chen, and Y. Luo, "A human ECG identification system based on ensemble empirical mode decomposition," *Sensors*, vol. 13, no. 5, pp. 6832–6864, 2013.

[44] Y. Chu, H. Shen, and K. Huang, "ECG authentication method based on parallel multi-scale one-dimensional residual network with center and margin loss," *IEEE Access*, vol. 7, pp. 51598–51607, 2019.
[45] J. Wu and Y. Zhang, "ECG identification based on neural network," in *Proc. 11th Int. Comput. Conf. Wavelet Act. Media Technol. Inf. Process. (ICCWAMTIP)*, Dec. 2014, pp. 92–96.

Chunyu Tan received the M.S. degree in mathematics from Wuhan University, Wuhan, Hubei, China, in 2015, and the Ph.D. degree in computer science from the University of Macau, Macau, China, in 2021.

She is currently a Lecturer with the School of Artificial Intelligence, Anhui University, Anhui, China. Her research interests include machine learning, biomedical signal processing, and e-health.

Liming Zhang (Member, IEEE) received the B.S. degree in computer software from Nankai University, Tianjin, China, in 1987, the M.S. degree in signal processing from the Nanjing University of Science and Technology, Nanjing, China, in 2000, and the Ph.D. degree in image processing from the University of New England, Armidale, NSW, Australia, in 2011.

She is currently an Assistant Professor with the Faculty of Science and Technology, University of Macau, Macau, China. Her research interests include signal processing, image processing, computer vision, and multimedia computing.

Tao Qian received the Ph.D. degree in harmonic analysis from Peking University, Beijing, China, in 1984.

From 1984 to 1986, he was with the Institute of Systems Science, Chinese Academy of Sciences, Beijing. He was also a Research Fellow with Macquarie University, Sydney, NSW, Australia, and held a post-doctoral position with the Flinders University of South Australia, Adelaide, SA, Australia, until 1992, under the supervision of A. McIntosh and G. Gaudry. As a Lecturer, he was with New England University, Armidale NSW, Australia, from 1992 to 2000. He has been an Associate Professor with the University of Macau, Macau, China, since 2000. He received the Full Professorship in 2003, and was the Head of the Department of Mathematics from 2005 to 2011. From 2013 to 2018, he was appointed as the Distinguished Professor of the University of Macau. Since 2019, he has been a Full Professor with the Macau University of Science and Technology, Macau. His research interests include pure analysis, applied and computational harmonic analysis, complex and Clifford analysis, signal analysis, and related areas.

Susana Brás received the Ph.D. degree from Abel Salazar Biomedical Sciences Institute, University of Porto, Porto, Portugal, in 2010.

She is a Researcher with the Institute of Electronics and Informatics Engineering of Aveiro (IEETA), University of Aveiro, Aveiro, Portugal. At her research unit, she has supervised several master's and Ph.D. students. She published several papers in top journals and conferences, which gave to her visibility in the scientific community, allowing the invitation to deliver several invited talks, internally and externally to the University of Aveiro. Her thesis was focused on automation in anesthesia. Her background is in applied mathematics from the Sciences Faculty, University of Porto, Porto, Portugal. Her research interests are focused on electrocardiogram (ECG) biometric identification, emotional modulated environments, and information extraction from large databases.

Armando J. Pinho (Member, IEEE) is a Full Professor at the Department of Electronics, Telecommunications and Informatics, University of Aveiro, Aveiro, Portugal, and a Researcher at the Information Systems and Processing Group, Institute of Electronics and Informatics Engineering of Aveiro (IEETA), where he is also the Current Director. His main research activity is in the area of data compression and associate data models, Kolmogorov complexity, and the applications of these concepts to problems in the area of computational intelligence.